2019

Biogeochemical Characterization of Metal Behavior from Novel Mussel Shell Bioreactor Sludge Residues

Sara C. Butler
University of Windsor

James Pope
CRL Energy Ltd.

Subba Rao Chaganti
University of Windsor

Daniel D. Heath
University of Windsor

Christopher G. Weisener
University of Windsor

geosciences

MDPI

Article

Biogeochemical Characterization of Metal Behavior from Novel Mussel Shell Bioreactor Sludge Residues

Sara C. Butler [1], James Pope [2], Subba Rao Chaganti [1], Daniel D. Heath [1] and Christopher G. Weisener [1,*]

[1] Great Lakes Institute for Environmental Research (GLIER), University of Windsor, Windsor, ON N9B 3P4, Canada; butle11j@uwindsor.ca (S.C.B.); chaganti@uwindsor.ca (S.R.C.); dheath@uwindsor.ca (D.D.H.)
[2] CRL Energy Ltd., Christchurch 8024, New Zealand; J.Pope@crl.co.nz
* Correspondence: weisener@uwindsor.ca

Received: 6 December 2018; Accepted: 9 January 2019; Published: 18 January 2019

Abstract: Acid mine drainage (AMD) remediation commonly produces byproducts which must be stored or utilized to reduce the risk of further contamination. A mussel shell bioreactor has been implemented at a coal mine in New Zealand, which is an effective remediation option, although an accumulated sludge layer decreased efficiency which was then removed and requires storage. To understand associated risks related to storage or use of the AMD sludge material, a laboratory mesocosm study investigated the physio-chemical and biological influence in two conditions: anoxic storage (burial deep within a waste rock dump) or exposure to oxic environments (use of sludge on the surface of the mine). Solid phase characterization by Scanning Electron Microscopy (SEM) and selective extraction was completed to compare two environmental conditions (oxic and anoxic) under biologically active and abiotic systems (achieved by gamma irradiation). Changes in microbial community structure were monitored using 16s rDNA amplification and next-generation sequencing. The results indicate that microbes in an oxic environment increase the formation of oxyhydroxides and acidic conditions increase metal mobility. In an oxic and circumneutral environment, the AMD sludge may be repurposed to act as an oxygen barrier for mine tailings or soil amendment. Anoxic conditions would likely promote the biomineralization of sulfide minerals in the AMD sludge by sulfate reducing bacteria (SRB), which were abundant in the system. The anoxic conditions reduced the risk of trace metals (Zn) associated with oxides, but increased Fe associated with organic material. In summary, fewer risks are associated with anoxic burial but repurposing in an oxic condition may be appropriate under favorable conditions.

Keywords: acid mine drainage; bioremediation; microbiology; mussel shells; mesocosm; contaminate waste storage

1. Introduction

Acid rock drainage (ARD) is a naturally occurring process that is amplified by mining activities and becomes an anthropogenic point source of pollution referred to as acid mine drainage (AMD) that commonly has a pH of <4. The geochemistry of waste rock will determine the specific contaminants in AMD, but can include high concentrations of Fe, Sulfate, Cu, Zn, Mn, Mg, Hg, As, Pb, and other metals. AMD affects many ecosystems around the world, both aquatic and terrestrial [1,2] and occurs when waste rock containing sulfides are oxidized, producing ferric iron (Fe^{3+}) which can act as an oxidizer in the absence of oxygen [3]. Surrounding streams can be contaminated by AMD and precipitates (such as schwertmannite and ferrihydrite) and, if not properly managed [4,5], will have toxic effects on benthic organisms [6]. Rates of AMD reactions can increase in the presence of bacteria [7] as microbes oxidize hydrogen sulfide produced during the dissolution of sulfide minerals producing sulfuric acid [8].

Remediation of AMD is traditionally divided into two categories: passive and active systems. Active systems involve the continued addition of alkaline substances to increase the pH and have higher capital and operational costs relative to passive treatments. Passive remediation refers to the use of wetland systems, both natural and manmade, and usually requires little maintenance and comparatively lower costs, making it the preferred choice for legacy sites or sites at closure. A novel full-scale mussel shell bioreactor (MSB) was constructed in 2011 and is currently treating an AMD seep at a coal mine on the west coast of the South Island of New Zealand. The MSB removes approximately 99% of all metals and raises the pH from 3.3 to 7.9 and is estimated to be 15 times more cost-effective than other methods [9]. The MSB has distinct geochemical layers including: an allochthonous sediment/sludge layer (0–15 cm), Fe oxide reacted shell layer (15–35 cm), Al oxide reacted shell layer (35–60) and reduced unreacted shells (60–130 cm). The efficiency of the reactor has decreased with time due to the build-up of fine-grained sediment and AMD remediation byproducts, referred to as sludge. This reflects a common problem in AMD remediation strategies: dissolved mine contaminant effluents are treated, but sludge is produced in large quantities, creating the need for a multi-step maintenance plan.

Traditional methods of AMD neutralization can produce up to 135,000 tons of AMD sludge per year from both passive and active technologies [10]. Few studies have examined the weathering and leaching behavior of these by-products, and there are even fewer on the effects of microbial activity on these materials. A review of sludge management practices found that the most common storage practice was within a sludge pond [10]. Other methods of management included mixing sludge with other tailings or waste rock dumps, pit disposal, or reusing it within the mine (such as using it for neutralization strategies). Some other recent applications of AMD sludge include mixing it with natural soils as an oxygen barrier for the storage of mine tailings to reduce further production of AMD [11]. Other studies explored the possibility of recovering elements of economic interests as well as classifying the risk associated with sludge storage [12]. Some concerns regarding sludge storage by mines listed in a review by Zinck and Griffith [10] were: space for disposal, the long-term stability of the sludge, and that sludge management requires a site-specific approach. The sludge in this study presents a unique problem as the downflow MSB is based on novel technology still being tested. In addition, this sludge is potentially acid-forming, while other AMD sludges may be alkaline.

The sludge layer has accumulated over a four-year period and has significantly impacted the performance of the existing MSB. The sediment sludge layer was found to contain gibbsite (an aluminum hydroxide), ferrierite, and have a pH of 3 [13]. The top sludge layer was removed in 2016 to increase the permeability and lifespan of the MSB. As part of their reclamation strategy, the mine site is currently interested in the behavior and functionality of the sludge. This study is focused on the upper sludge layer and presents the geochemical stability in two potential storage environments, oxic and anoxic with and without the influence of microbes. The purpose of this study is to determine if this sludge may be able to be used for further mining management, such as repurposing with soil blends, and if not, how the sludge will behave if stored in an anoxic environment. The anoxic incubation also provided a way to test if the microbial community from the oxic portion of the bioreactor could thrive in an anoxic environment and if they would increase the stability of the sludge. In this study, we investigate the physicochemical and biological influence of an AMD sludge layer under conditions of anoxia and oxygen saturation. A series of laboratory mesocosms were designed to simulate aerobic and anoxic storage/disposal options and to characterize the chemical and biological stability. Here we determine oxygen and hydrogen sulfide diffusive flux, metal stability, and microbial community drivers which can impact the sludge stability in the presence/absence of oxygen as a function of aging.

2. Materials and Methods

2.1. Site Description and Laboratory Incubations

Details of the MSB and mine site have been described in past studies [9,13–15]. The coal mine is located on the west coast of New Zealand within the Brunner Coal Measures, a formation containing 1–5 wt% pyrite and is potentially acid forming (PAF) [14,16,17]. This resulted in AMD runoff high in Fe and Al as well as trace metals including As, Cd, Ni, Pb, Tl, and Zn [15,18,19]. Numerous on-site management practices are currently in place, including: active treatment using CaO to neutralize AMD, barrier systems to exclude oxygen and water, and strategic mine planning, which is summarized in DiLoreto et al., (2016b). The MSB was built with 362 tons of mussel shells which have a range of 88–95 wt% $CaCO_3$ with the remaining weight made up of organic material and has been treating an AMD seep since late 2012. Since then it has undergone two sampling periods over two years where it was characterized both microbially and geochemically [9,13].

Bulk sediment samples were collected from the first 10 cm (sediment/sludge layer) of the MSB in February 2016, as well as mine water, which was obtained from the inlet of the MSB. The samples were stored and shipped under refrigeration to minimize geochemical alterations until experimental set up. A 2 × 2 experimental design (with replicates) allowed two environmental conditions (anoxic and oxic) to be tested, and determined the microbial impact (biotic vs. abiotic) on the sludge. This study design has been used in numerous past studies to address environmental impacts of various materials [20–22]. The four experimental conditions discussed in this study are biotic anoxic, abiotic anoxic, biotic oxic, and abiotic oxic. Differences between the abiotic and biotic mesocosms are referred to as microbial effects, while variations between the anoxic and oxic mesocosms are referred to as atmospheric effects. Sediment and water for the abiotic mesocosms were sterilized by gamma irradiation at the McMaster Institute of Applied Radiation Services (McIARS) in Hamilton, Ontario, Canada. An anaerobic chamber achieved anoxic environmental conditions, filled with approximately 95% N_2 and 5% H_2, and with moisture control. The oxic mesocosms were left in the natural laboratory atmosphere, just outside the chamber. All mesocosms were duplicated and covered by black fabric to allow minimal light interference. These mesocosms mimicked conditions of deep burial and/or anoxic ponds as well as storage on the mine surface (oxic). Approximately 2 kg of sediment and 1 L of cap water (AMD water from inflow of the MSB) was placed in sterilized 4 L Camwear® containers with lids (but not airtight) from the Cambro Manufacturing Company. Sediment samples were taken after approximately 4, 12, and 20 weeks for microbial analysis from the surface of the sludge within the mesocosm (first 1 cm). A spatula was used to collect samples from different sections during each sampling period, as to not sample an area which was previously disturbed. Final samples (approximately 15 g) from the top 1 cm of the sediment, near the center of the mesocosm, were collected for geochemical analysis. This included solid phase analysis using a scanning electron microscope and selective geochemical extractions.

2.2. Microsensors and Diffusive Flux Calculations

HS^-, O_2, and redox microelectrode sensors (Unisense Science, Denmark) were used to measure vertical gradients approximately 1 cm above and 1 cm below the sediment water interface, a method developed by Revsbech, (1989) [23] but more explicitly following methods by Reid et al. (2016) [20]. The sensor measurements were taken near the center of the mesocosm, and before each sediment sampling period, so the profiles would be undisturbed. Sensor manipulation was done via a computer fitted with SensorTrace Pro software and the Unisense Microsensor Multimeter model PA2000. The microsensors have 10(H_2S)-500 (oxygen) μm glass tips and take precise and continuous measurements using an automated micro manipulator, able to take measurements every 100 μm. Calibration and pre-polarization guidelines followed the Unisense prescribed procedures [24]. Profiles were taken at 4 and 20 months during the incubation for every mesocosm.

A diffusivity sensor (50 µm) was used to measure diffusivity constants in all mesocosms at the end of the incubation period. This required using a two-point calibration [25] and an inert gas, in this case, 5% H_2 mixed with 95% N_2. A slope derived from the profiles of O_2 and H_2S^- is used along with the diffusivity measurement in the following equation:

$$J(x) = -\varnothing D(x) \frac{dC(x)}{dx} \ [\mathrm{cm^2 S^{-1}}] \quad (1)$$

$J(x)$ is flux; $-\varnothing D(x)$ is the diffusivity measured using the diffusivity sensor on the sediment; and $dC(x)/dx$ is the slope of the HS^- and O_2 concertation profile measured along the sediment-water interface.

2.3. Geochemical Phase Description

2.3.1. Scanning Electron Microscopy (SEM) and Particle Count Analysis

Solid samples collected from the initial bioreactor sediment (time zero) and final timepoints were preserved (approximately 5 g) and made into polished thin-sections for mineral characterization by Scanning Electron Microscopy (SEM). The analysis was completed to determine geochemical differences in the sediment after incubation in oxic and anoxic conditions, and to determine any microbial effects (differences between biotic and abiotic). Analyses were performed using a FEI Quanta 200F, Environmental Scanning Electron Microscope (FEI, Eindhoven, The Netherlands) at high vacuum (20 kv) with a theoretical spot size of 2.6 nm, at the Great Lakes Institute for Environmental Research (GLIER), University of Windsor, (Windsor, ON, Canada). Visual inspections of mineral grains were completed using both backscattered electron (BSE) and secondary electron detectors (SE). The SEM was configured with an EDAX® SiLi detector (EDAX, Mahwah, NJ, USA) to analyze differences in the elemental composition of mineral grains in each mesocosm. EDAX Genesis Particle cluster analysis software (version 5.21) was used for particle counts and elemental composition. Duplicate areas were analyzed on each thin section at 1000× magnification to account for particles sizes down to 1 µm. Particles were identified by the software and counted based on their brightness under constant levels of contrast for every sample. This allowed for only particles of heavy elemental weight to be counted for the following elemental proportions: C, O, Mg, Al, Si, S, K, Ca, Ti, Mn, Fe, Co, Cu, and Zn. Data for Figure 1 was normalized to 100% for Fe, S, and O to determine the presence of iron sulfides and iron oxides; however, all concentrations discussed in the text are normalized values for all elements selected on the EDAX detector.

2.3.2. Selective Solid Phase Extractions

In total, five geochemical extractions were completed on the final incubation samples to be compared with the initial sediment. Sediment was collected from the top 1 cm of the sludge using sterilized spatulas and put into sterilized 50 mL polypropylene centrifuge tubes (in triplicates). Samples were also taken from the top of the MSB to act as a time zero. All extractions were done using a 1:10 ratio of sediment to extractant fluid, specifically 3 g to 30 mL. The five extraction targets were as follows: water-soluble; bio-available (EDTA); amorphous oxyhydroxide phases (reducible); strong acid extractable; and metals weakly bonded to oxide phases (weak acid) following the same protocols as Diloreto [26] and described in Table 1. The sediment and extractant fluid within the tubes were shaken (using an oribital shaker) for 24 h, except for the strong acid extraction which was shaken for 21 days to achieve total extractable. The extractant fluid was filtered, acidified (for preservation), and then analyzed using a 700 series Agilent 720-ES ICP-OES system for heavy metals. Principle component analyses (PCA) were used to evaluate the chemical extraction data to determine the variation between experimental factors and the elements with the most substantial impact on each representative environment. Initial samples from the MSB were also included in the PCA and will serve as a time point zero, referred to as "initial". PCA analysis also determined microbial effects based

on clustering and PC scores; if the abiotic incubation clustered separately from the biotic, then it was considered to have microbial effects. Using PAST, two-way ANOVA tests were also used to determine atmospheric or microbial effects on specific metals in each geochemical phase. Student t-tests were performed within Excel on individual samples to determine if significant differences existed between geochemical phases in the abiotic vs. microbially active incubations.

Table 1. Selective geochemical extractions used.

Target	Extractant	Citation
Water-soluble	N purged milli Q water	Ribeta et al. (1995) [27]
Bio-available	0.005 EDTA adjusted to pH 6	Fangueio at al. (2001) [28]
Metals weakly bonded to oxide phases	0.5 M HCl	Heron et al. (1994) [29]
Amorphous oxyhydroxide (reducible)	0.12 M sodium ascorbate; 0.17 M sodium citrate; 0.6 M NaHCO3, adjusted to pH 8	Amirbahman (1998) [30]
Strong acid extractable	5 M HCl	Heron at al. (1994) [29]

2.4. Microbial Community Analyses

2.4.1. DNA Extraction and Sequencing Preparations

Sediment samples (approximately 1 g) were collected for three-time points throughout the five-month incubation in triplicate from the first 1 cm of sediment from the laboratory incubation and stored at −80 °C. The initial samples collected from the field were flash frozen, stored in liquid nitrogen, and transported to a −80 °C freezer. DNA extractions, using 0.25 g of sample, were performed using MoBIO power soil DNA kits (Mobio Laboratories, Carlsbad, California) according to manufacturer protocols. Two-step PCRs were completed to amplify and barcode the DNA, according to the protocols laid out in Falk et al. [31]. However, in the current study, the V4–V5 regions of the 16 s rRNA gene were amplified with the initial PCR using primers 515F-Y and 926R [32]. Amplified DNA products were then individually barcoded by the sample (PCR 2), pooled according to band intensity by gel electrophoresis, and analyzed on the Agilent 2100 Bioanalyzer (Agilent Technologies, Santa Clara, CA, USA) for quality and quantity determination. The pooled sample library was then sequenced on the Ion Torrent Personal Genome Machine (Life Technologies, Carlsbad, CA, USA) at GLIER, University of Windsor, Canada.

2.4.2. Community Structure Analysis

Microbial taxonomic identification was completed using the MacQiime 1.9.1 (Quantitative Insights into Microbial Taxonomy) pipeline (http://qiime.org/). The raw sequence file was demultiplexed, barcodes/adapters were removed, and sequences filtered for quality assurance. Sequences were cut off at a Phred score of 25, samples were removed with sequence counts less than 3000, and chimera sequences were identified and removed using usearch61 [33]. Clustering of sequences into operational taxonomic units (OTUs) was performed by open-reference OTU using a 97% similarity threshold with the uclust algorithm [34]. Taxonomy was also assigned by uclust, with a 90% consensus threshold, using the default GreenGenes database and normalized using DESeq2 [35], as this method is acceptable for low replicate studies (<20) [36].

Diversity indices were computed using the Shannon-Wiener [37] and Chao indices [38] using the alpha diversity scripts by MacQiime. This determined if oxic or anoxic incubation environment altered diversity. Rarefaction curves were also produced using scripts within MacQiime, with sequences greater than 3000. Principal coordinates analysis (PCoA) was conducted using the R package for Amplicon-Sequencing-Based Microbial-Ecology (RAM) v1.2.1.3 on the top 1000 OTUs representing 80% of the total sequence reads for all samples. PCoA was used to determine if major differences

existed between oxic, anoxic (all time points), and initial communities based on clustering. Further, microbial community differences between the oxic and anoxic mesocosm differential abundance analysis were assessed at an OTU level. Differential abundance of OTUs was computed using the DESeq2 method [35].

In order to predict the broad functional changes in microbial diversity in oxic and anoxic environments, differences at the phylum level were examined. To determine major changes that are not detected at the phylum level, the top 15 classes that incorporate 80% of the sequences were analyzed. Differential abundance (described above) was also used to validate broad differences observed by relative abundance alone.

To compare the influence of environmental and chemical factors on the microbial diversity in oxic and anoxic environments, Canonical Correspondence Analysis (CCA) was used. Instead of using the individual metals for each geochemical phase, PC loadings from the PCA described in Section 2.3.2 were used as the environmental factors. The top 1000 OTUs, representing 80% of the total sequences, were used as the microbial response for the CCA plot.

3. Results and Discussion

3.1. Oxygen and Hydrogen Sulfide Flux

The diffusive flux of both oxygen and H_2S were determined for the oxic and anoxic sludge incubations treatments respectively. Oxygen and hydrogen sulfide concentrations were measured in each mesocosm across the sediment-water interface to determine the concentration gradient. The abiotic incubations showed DO at 5.5–7.5 mg/L, which decreased to zero within 1 cm past the sediment-water interface (Table 2). In comparison, the biotic incubations showed less oxygen in the cap water with ~2–3 mg/L rapidly decreasing to 0 mg/L ~0.5 cm into the sediment. Oxygen concentrations are higher in the abiotic system as microbes produce reducing agents and consume oxygen. These oxygen profiles and apparent diffusivity (porosity*diffusivity coefficient) were used to calculate flux. The redox potential across the sediment interface was also measured. ORP values remained consistent ranging from 262 (eV) to 229 (eV) in the oxic treatment over five months. In contrast, the anoxic treatments showed the development of reducing conditions (Table 2).

Table 2. Chemical and physical properties of sediment (diffusivity and flux) and water cap (pH) for all incubations for each month sampled. Each number represents an average for each experimental condition. ND (not detected) was recorded for certain samples as oxygen was not present in the Anoxic, and H_2S was not found in the abiotic mesocosms or the oxic.

Chemical Component	Month	Oxic		Anoxic	
		Biotic	Abiotic	Biotic	Abiotic
oxygen flux [1]	1	1.83	2.79	ND	ND
	5	1.21	6.23	ND	ND
H_2S flux [1]	1	ND	ND	210	ND
	5	ND	ND	60.9	ND
O_2 (mg/L)	1	2.6	5.5	0	0
	5	3.01	7.1	0	0
HS (µmo/L)	1	0	0	8.7	5.96
	5	0	0	15	ND
Redox Potential	1	262	230	10	80
	5	229	300	−80	−100
pH	1	3.27	4.1	5.89	5.92
	5	3.24	3.74	5.19	4.87

[1] units: mmol m^{-2} day^{-1}.

In comparison to the abiotic, the calculated oxygen flux within the biotic incubations did not have a large shift from the first month to the final (from 1.21 to 1.83 mmol m^{-2} day^{-1}). Oxygen flux in the abiotic mesocosm increased from 2.79 mmol m^{-2} day^{-1} to 6.23 mmol m^{-2} day^{-1} based on the first and final month. These flux values were low compared to natural systems which have been reported up to 89 mmol m^{-2} day^{-1} in productive lakes [39]. In the biological system, oxygen was consumed during the formation of minerals observed at the interface very early on in the mesocosm experiment (within one month). The system reached a steady state quickly and therefore the biological and chemical demand for oxygen was low, though oxygen was still being consumed. The diffusivity constant was approximately 75% lower in the biotic mesocosm which may have been caused by the increase of iron oxides (possibly amorphous) which altered the porosity and the sediments ability to diffuse oxygen. This was supported by visual observations during the first month of the mesocosm, in which a bright orange precipitate formed on the surface of the sludge in the biotic trials. In the abiotic system, the higher diffusion coefficient allowed for significant diffusion of oxygen into the sediment compartment, uninhibited by biological consumption of oxygen. In this case, the biotic oxygen flux had a much steeper slope over a shorter depth. The difference in oxygen concentration in the overlying water was higher for the abiotic system, and resulted in a shallower depth concentration gradient. Observations of the abiotic system showed a change in sediment color at around four months, suggesting that at this time the sediment had oxidized at a slower rate than what was observed in the biotic system.

Under conditions of anoxia, a primary concern regarding sulfide-rich sludge is the evolution of hydrogen sulfide. To determine the potential flux of hydrogen sulfide from the MSB sludge, several measurements were collected using the biotic and abiotic incubated materials. The abiotic incubations showed no significant H_2S and therefore no flux was calculated. In contrast, the anoxic biotic incubations showed an elevated concentration of 8.7 µmol/L hydrogen sulfide at 1 cm below the sludge/water interface. The calculated hydrogen sulfide flux for both the first and final time points showed a decrease in H_2S concentration from 210 to 60 mmol m^{-2} day^{-1}. Although no increase in H_2S was observed in the water cap of these experiments, it suggests that the observed decrease of measurable sulfide flux may in part be due to secondary processes (e.g., sulfide precipitation or a decrease in sulfur reducing bacteria). This result is similar to those found in Reid et al. [21] and was suggested to be related to the formation of sulfides causing an increase in porosity. Sulfides, such as FeS_2 have a defined crystalline cubic structure. However, when produced by microbial metabolic activity, they can occur as framboidal pyrite. Framboidal pyrite has an increased reactive surface area [17] which could affect the porosity and diffusive flux in the sediment. The H_2S flux calculated for the anoxic incubations showed a decrease in flux over time, which suggests that H_2S was not as easily diffused out into the water column and is being sequestered into the sediment.

3.2. Geochemical Phase Classification Using Two Methods to Quantify Microbial and Atmospheric Effects

3.2.1. Biomineralization (Sulfide) Characterization in Oxic and Anoxic Environments Using Scanning Electron Microscopy (SEM)

A modal investigation of the iron and sulfur mineral phases for the abiotic and biotic conditions was performed using SEM particle analyses. The proportion of sulfur and iron-bearing phases was determined from a total population of 1000 grains in which elemental ratios were defined. Particles with a high percentage of sulfur and iron were categorized as pyrite or potentially greigite, a precursor to pyrite framboids [40], and compared to the proportion of iron oxide particles. Based on the elemental analyses for each particle, a strong contrast between the proportion of iron and sulfur-rich (<10% total modal percentage) particles were observed in the biotic incubations compared to the abiotic under anoxic conditions (Figure 1). The proportion of sulfide particles observed in the biotic incubations (higher percentages of iron and sulfur) make up 4% of all the particles analyzed for the anoxic biotic incubations. SEM micrographs in Figure 1 show an aggregation of submicron microcrystals with a Fe:S ratio of 1:1. These measurements suggest the formation of monosulfides (e.g., Greigite, Mackinawite), which are precursors to pyrite formation and are known to be associated with microbial activity [40–42].

These will most likely be replaced by pyrite if conditions persist and are formed from H_2S, which is produced by sulfsulfate reducing bacteria. [40]. The chemical profiles suggest that H_2S is most likely being sequestered into aggregates of sulfide within the sediment. These particles in the abiotic incubation make up only 0.3% of the particles analyzed for the abiotic incubations and 1.8% from the initial top sediment sludge. This suggested that the microbes were vital in the formation of iron sulfides in storage environments. In the oxic condition, there were fewer particles with high sulfur concentrations for both biotic and abiotic incubations, though a large proportion had high iron concentration. These high iron, but low sulfur particles are most likely iron oxides.

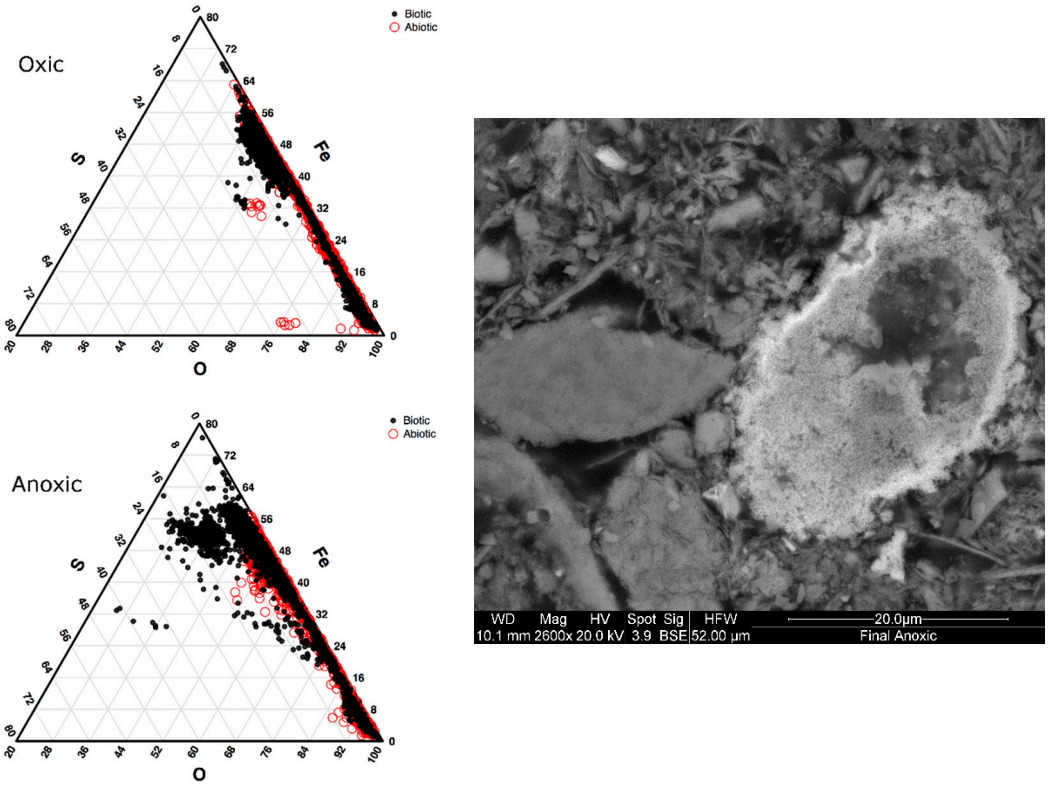

(**a**) (**b**)

Figure 1. SEM analysis of sludge collecting from final sediment samples; (**a**) Ternary plot shows the distribution of Fe, S, and O elemental concentrations. The oxic incubations are shown on the top figure and anoxic on the bottom, with data from the biotic incubations represented by solid black circles and the abiotic data represented by open red circles; (**b**) Example of a high sulfur and iron particle showing submicron microcrystals in a pre-framboidal texture.

3.2.2. Solid Phase Characterization and Metal Behavior, Using Principal Component Analyses (PCA)

Five solid phase extractions (e.g., water soluble, amorphous oxyhydroxides, weakly bound iron oxide phases, those prone to biological complexations, and strong acid extractable) were used to target metal solubility within the sludge material as a function of treatment. The PCA along with ANOVA analyses determined which metals within each mineralogical phase were susceptible to either biotic or abiotic geochemical alteration in both the presence and absence of oxygen. Only the amorphous oxyhydroxide phase were susceptible to microbial effects, while the other four phases were more strongly affected by the presence or absence of oxygen, based on differences between oxic and anoxic incubations. Those four geochemical phases were not altered by the presence or absence of microbial activity e.g., no new secondary mineral phases produced.

The targeted amorphous oxyhydroxide phase (i.e., easily reducible) within the sludge was susceptible to both microbial and atmospheric effects based on a PCA analysis and ANOVA. Analyses of all four mesocosm conditions showed distinct variation as each reported to separate quadrants (Figure 2). 54% of the variance was explained by PC 1 and 27% of the variance was explained by PC 2, both of which are significant based on a 999-repetition row-wise bootstrap analysis. Both components had strong loadings from Fe, S, Al, and Ca with PC 2 suggesting an inverse relationship between Fe and S. Based on the scatter plot, it appears that PC2 shows microbial influence on the amorphous geochemical phase with the abiotic incubations both plotting positively, and the active incubations plotting negatively. The ANOVA analysis supports this as well, showing a significant variance of Fe concentrations in this phase which suggests microbial and atmospheric effects. The Fe concentrations in this amorphous phase in the biotic oxic incubation (1400 ± 300 mg/kg) are approximately 1.5× greater than within the abiotic. These phases include amorphous iron oxyhydroxides such as ferrihydrite, which is commonly found in AMD environments and is associated with microbes [43]. Ferrihydrite can be formed directly by the oxidizing of Fe(II) by bacteria, or the bacteria can act as a nucleation site with mineralization of iron oxides encompassing both dead and living cells [43]. Since amorphous iron oxyhydroxides are also involved with the adsorption of trace metals [44–46], an unstable environment for these mineral phases would cause other types of contaminants common in the mine to be released in addition to Fe.

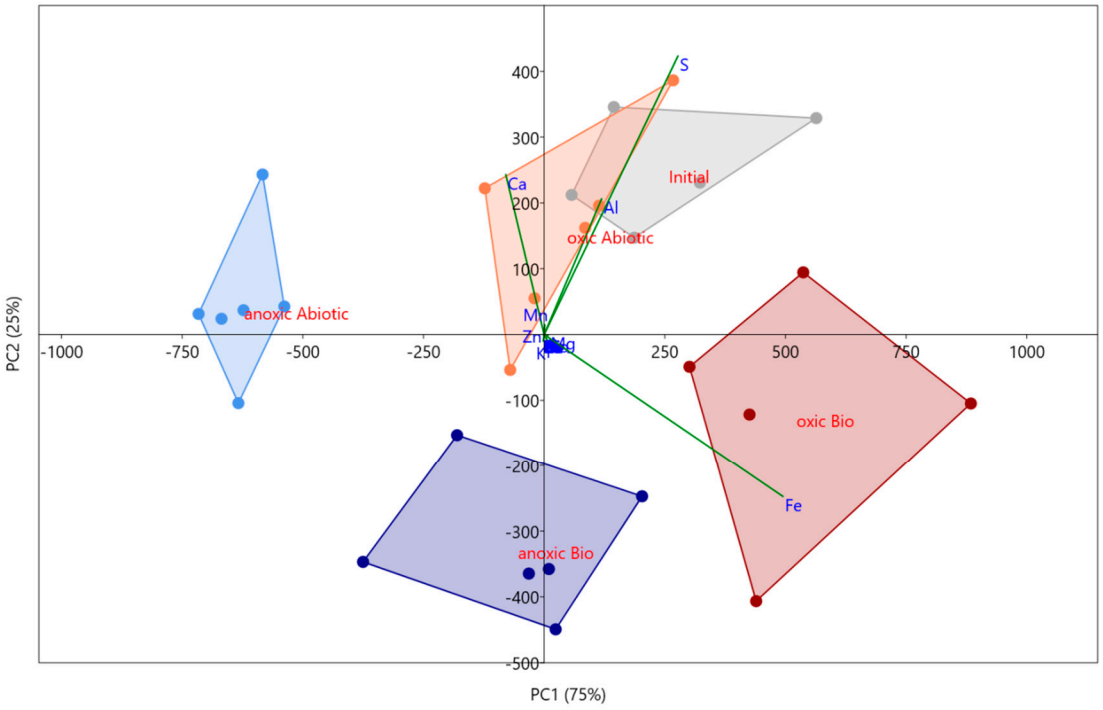

Figure 2. PCA scatterplot for the Oxyhydroxide mineral phases in all four experimental conditions and the initial in situ sediment from the MSB. PC1 represents 77% of the variance, while PC2 represents 20%. Convex hulls are connecting sample groups labelled on the figure, generated in PAST.

Other targeted phases included organically bound, water soluble, metals weakly bound to oxides, and strong acid extractable (total metals) phases. All followed a similar trend, with the atmospheric effects having a greater influence than the microbial effects. The variation in these geochemical phases was based on both PCA and ANOVA. For these phases, PC 1 explains >90% of the variance, and apart from the water-soluble phase, they all had strong loadings of Fe. In the water-soluble phase, PC 1 had loadings of Ca, S, and Mn. Concentrations within water-soluble fractions were lower in the anoxic mesocosm compared to the oxic for S (150 ± 15 compared to 250 ± 15 mg/kg) and Mn (10 ± 1 kg compared to 40 ± 5 mg/kg). This suggested higher stability in anoxic conditions concerning possible

contaminants such as Mn and S. Other contaminants such as Zn (~0.2 mg/kg) and Mg (~25 mg/kg) were not significantly different between atmospheric effects, and Fe is not contained within any water-soluble phases. Compared to Mn and S, Zn, Mg, and Fe had no impact on the stability of the sediment based on the water-soluble phases.

The organically bound, weakly bound to oxides, and strong acid extractable phases all had strong loadings of Fe. The organically bound Fe concentration in the oxic mesocosm was 90 ± 20 (abiotic) and 210 ± 70 mg/kg (biotic) with no significant difference between abiotic and biotic in the anoxic conditions (2300 ± 300 mg/kg). Under anoxic conditions, Fe(II) will form colloids with organic matter and may be mobile in organic-rich systems based on a laboratory study [47]. In a typical AMD or mine environment, organic matter may not be high, but previous studies suggest that mixing with soils under anoxic conditions may increase the chance of stable colloid formations, which may be easily transported downstream [40]. Iron was not contained in the weakly bound oxides phase in the anoxic mesocosm, though the oxic had 2700 ± 200 mg/kg in the biotic and slightly less (2200 ± 300 mg/kg) for the abiotic. There were fewer oxides in the anoxic mesocosm overall, and iron may be preferentially adsorb to organic matter in the anoxic condition, rather than any oxides present.

Although Zn did not have strong loadings in any of the geochemical phases tested based on the PCAs, it is identified as an element of concern for the mine. Based on this study, up to 33 ± 5 mg/kg of zinc could be in the initial sediment across all mineral phases, though this decreases to 21–27 mg/kg after all incubations, suggesting that some Zn was possibly unaccounted for in the extractions or went under dissolution into the water column. Besides total extractable metals, the highest concentration of Zn was found in the extraction targeting sorbed metals to poorly crystalline phases, which was found to vary significantly by atmospheric condition (17 ± 4 mg/kg in the oxic and between 4–7 mg/kg in the anoxic). Zn will most likely be adsorbed or coprecipitated with oxyhydroxides [45,46] in the oxic mesocosm. In this case Zn will be insoluble in water, based on the soluble phase phases' extractions (<0.5 mg/kg measured). Other mineral phases had concentrations of zinc less than 2 mg/kg with no significant microbial or atmospheric effects.

3.3. Community Structure Shifts as a Function of Anoxic and Oxic Incubation Environments

To determine correlated factors controlled by microbial effects, 59 samples were analyzed for the microbial community, detecting over 500,000 quality sequences with an average of 8793 sequences per sample. Sequences within samples ranged from 3000–20,294 (after a low-read cut-off) and were clustered into 14,489 OTUs. Between the oxic and anoxic communities, there were 137 OTUs out of 14,489 OTUs identified as significantly differentially abundant (adjusted p-value less than 0.05). The majority of these OTUs (97/137) are highly abundant in the oxic incubations and represent 18.3% of the normalized (DeSEQ2) sequence counts. The OTUs that are overrepresented in the anoxic incubations represent 8.7% of the normalized sequence counts from samples in the anoxic time point. Rarefaction was completed on samples with over 3000 sequence hits at 10 iterations to determine species richness. Curves produced did not completely plateau, suggesting that full coverage was not reached, though for many samples it appeared to be close. Shannon and Chao1 indices were used to determine microbial diversity using the rarefaction cut-off of 3000. Diversity was slightly higher in the oxic incubations compared to the anoxic atmospheric environments, though neither were significantly different from the initial sediment (Table 3).

A PCoA suggested a community shift for both oxic and anoxic communities (Figure 3). All samples that were incubated plotted in the positive quadrants of PC 1 & 2 with samples from months 3 and 5 overlapping for both oxic and anoxic mesocosm. The final timepoints plotted separately and suggested a shift in the community later in the incubation that created a more unique community for the anoxic mesocosm. For this reason, the rest of the results will focus on the final timepoints to determine major long-term differences in the microbial community for oxic and anoxic storage. This will also allow for direct comparisons to geochemical phases as these were collected at the end of the incubations.

Table 3. Alpha rarefaction showing average diversity metrics for the time points of each incubation with the standard deviation between the replicates and the iterations shown.

	Months	Chao	Shannon	Observed Rarefied OTUs
	Initial	2065 ± 200	7.5 ± 0.2	930 ± 50
anoxic	1	2199 ± 100	7.71 ± 0.03	960 ± 10
	3	2184 ± 300	7.4 ± 0.5	920 ± 100
	5	1479 ± 60	7.5 ± 0.4	810 ± 100
oxic	1	2618 ± 100	8.2 ± 0.1	1130 ± 40
	3	2243 ± 200	7.7 ± 0.1	960 ± 40
	5	1732 ± 200	7.6 ± 0.3	850 ± 100

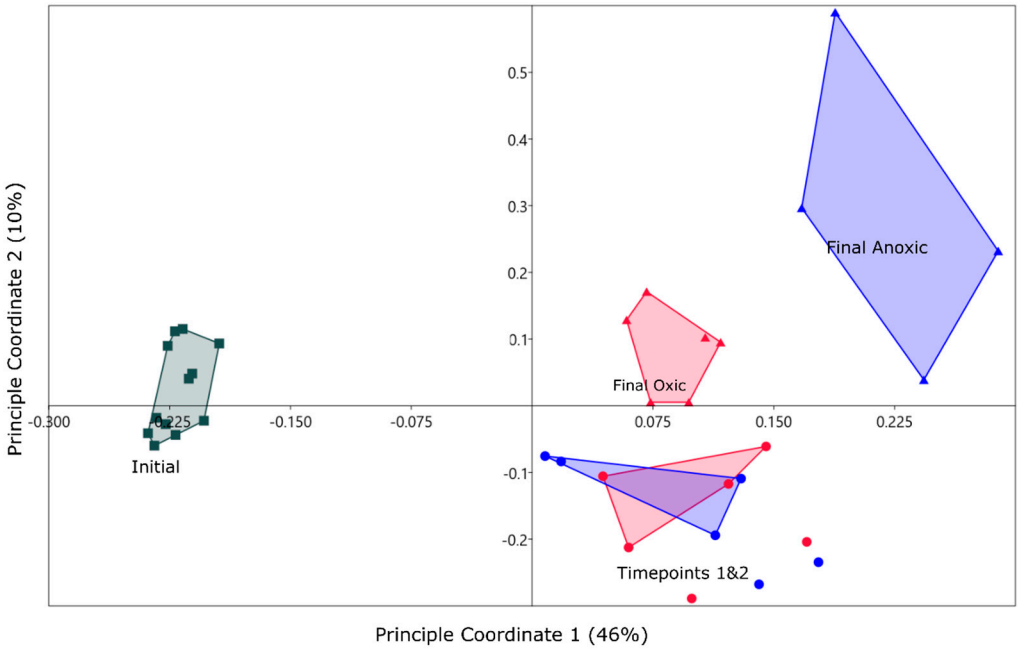

Figure 3. PCoA of the top 1000 OTUs from the initial (squares), oxic (red) and anoxic (blue) incubations. Final timepoints (month 5) are represented by triangles for both atmospheric conditions. Coordinate one represents 46% of the variance and coordinate two represents 10%. Convex hulls are connecting sample groups on the figure, done within PAST. Timepoints one and two represent month 1 and 3 sampling periods.

PCoA suggested a shift from the initial community in the bioreactor based on an input of OTUs which needed to be classified into taxonomic groups in order to put context into the changes observed. OTUs in the initial samples were identified to be from the following phyla: *Proteobacteria* (40%), unassigned (12%), *Acidobacteria* (12%), *Chloroflexi* (5%), *Planctomycetes* (5%), and *Actinobacteria* (5%), with other groups making up the remaining 21% and individually less than 5%. After incubation in an oxic condition, the community was similar to the initial community when looking at the distribution of phyla. Sequences were identified to *Proteobacteria* (30%), *Acidobacteria* (13%), *Bacteroidetes* (9%), unassigned (9%), *Chloroflexi* (6%), and *Actinobacteria* (6%) phyla and other groups contributing individually less than 5%. Sequences in the anoxic community sequences are divided into *Proteobacteria* (30%), *Firmicutes* (16%), *Bacteroidetes* (12%), unassigned (10%), *Acidobacteria* (6%), and *Chloroflexi* (4%). From a phylum perspective, the oxic mesocosm is closer to the initial community than the anoxic, apart from *Bacteroidetes* which increased in both oxic and anoxic mesocosms. The anoxic community was found to have an abundance of *Firmicutes*, which were initially below 5% in the MSB.

Based on the analysis of phyla alone, certain aspects appear unchanged by storage in anoxic conditions, specifically the *Proteobacteria* community. In initial, oxic, and anoxic mesocosms *Proteobacteria* is the dominant phylum, though after incubation the taxonomic classification at the Class level suggests a shift in the proteobacteria community related to atmospheric conditions. The top 15 classes (representing 70–80% of the normalized sequences), included *Gammaproteobacteria*, and *Alphaproteobacteria* which are abundant in the initial MSB community (20% and 11% respectively) with low abundance of *Deltaproteobacteria* (Figure 4). The oxic mesocosms appeared to be somewhat similar in composition to the initial, although the overall abundance of classes within *Proteobacteria* decreased. The anoxic community saw a large shift from a dominantly *Proteobacteria* community, to a more *Deltaproteobacteria* dominant community. Another class that was dominant within the anoxic community is *Clostridia* (*Firmicutes*), which was less than 1% of the initial community. OTUs that were identified as differentially abundant were also classified into *Deltaproteobacteria* and *Clostridia*, suggesting that both groups were unique to the anoxic mesocosm compared to the oxic, and may have impacted the geochemistry.

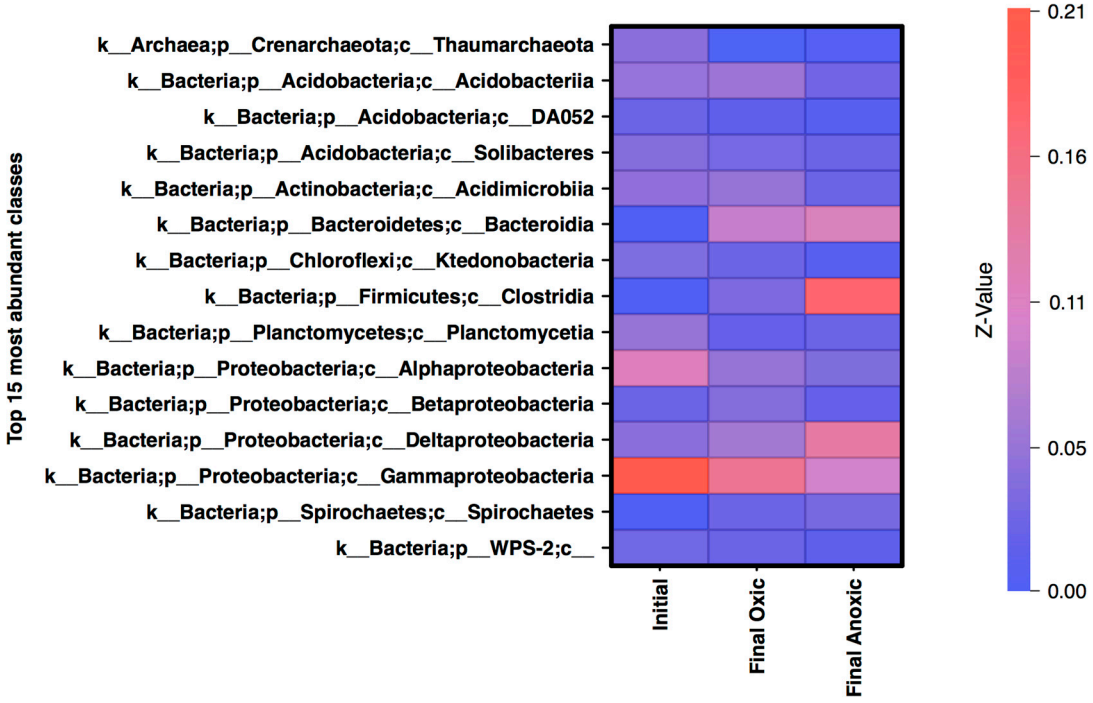

Figure 4. Heatmap of the relative abundance of normalized counts for the top 15 most abundant classes in the final timepoints and the initial samples with the relative abundance displayed on the y-axis, normalized to 1 for the total community. Most abundant classes are shown in red while the least abundant are shown in blue.

3.4. Biogeochemical Connections of AMD Sludge, and Associated Risks

To correlate the geochemical phases and the microbial community drivers for the biotic incubations, a CCA analysis was performed using the PC loadings from each geochemical phase (Figure 5). For all phases, except for the amorphous oxyhydroxide phase, only PC 1 was used as others were insignificant. Based on this CCA, PC 2 of the oxyhydroxide phase correlates with the community in the oxic condition. PC 2 had strong loadings of Fe, with a negative correlation to S, and based on the PCA scatterplot (Figure 2), controls the variance associated with the effects of microbes on this phase. Fe was sequestered in the sediment during incubation by microbes in the oxic phase, while mechanisms for sulfur sequestration in an oxic condition are unlikely at this pH and temperature. The bioavailable phase appears to correlate with microbial activity based on this CCA plot, however, based on the concentrations of Fe in this phase there is no significant difference between the biotic and abiotic

incubations. Fe may be bound to organic substances that were already present in the sediment such as organic material from the mussel shells and not affected by active microbes. All other phases do not appear to correlate to the three groups, which is supported by the PCA results, in that no biological effects were found for those phases.

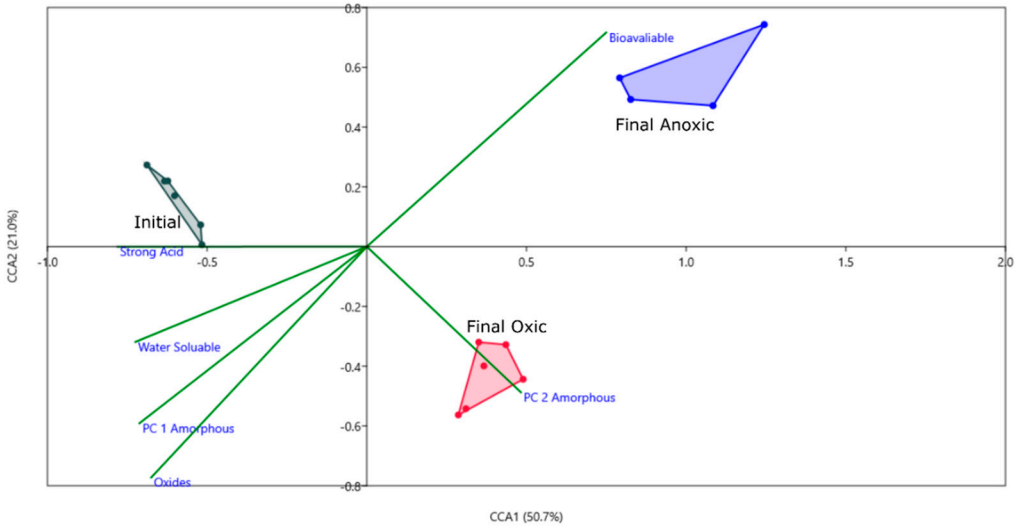

Figure 5. CCA plot using PCA components as environmental variables for each geochemical phase. PC 1 and PC 2 are included for the oxyhydroxide mineral phase as they are both significant, and only PC 1 is included for all other phases. Axis one represents 50% of the variance and axis 2 represents 21%. Convex hulls are connecting sample groups on the figure, done within PAST.

Based on the PCA, CCA, and particle analysis presented, there are significant geochemical differences based on oxic or anoxic incubation. Some of these differences can be attributed to microbial activity (observed microbial effects), such as the increased Fe in oxyhydroxide phases and counts of particles with high sulfur content (possible Greigite). For this reason, differential abundance was used to tease out differences between the oxic and anoxic community on an OTU level and to identify important groups that influenced geochemistry in each environment. Genera which are significantly differentially abundant in oxic and anoxic, and highly abundant in the initial MSB for comparison were shown in Figure 6.

Within the oxic incubation, OTUs classified as unidentified genera within the families of *Xanthomonadaceae*, *Acidimicrobiales*, *Ignavibacteriaceae*, and *Porphyromonadaceae* (*Plaudibacter*) were significantly differentially abundant compared to the anoxic environments. These differentially abundant groups may have been responsible for the further oxidation and increased production of amorphous iron oxyhydroxides as noted by the geochemical phase extractions and correlations based on the CCA plot (Figure 5). The family *Acidimicrobiales*, in particular, may have included the iron oxidizing species such as *Acidimicrobium ferrooxidans* [48], which could have been responsible for increased iron oxide production. Other highly abundant bacteria such as *Pseudomona* and *Bacteroidales* present in the incubation could be responsible for organic carbon degradation or act as a nucleation site for mineralization of hydroxides [43]. Iron oxides are insoluble in most neutral waters but could dissolve if in acidic environments [49]. In previous studies, acidic environments were shown to cause dissolution of AMD sludge and suggested soil mixing or a protective gravel layer [11,50]. The ability for the sludge to act as an oxygen barrier was also tested in this previous study which found a varying oxygen flux from 0–50 mmol m^{-2} day^{-1} over a period of two years in a column experiment. This study suggested that AMD sludge with low oxygen flux (<20) could be used as an oxygen barrier for other mine tailings or waste rock with soil mixing and water cover [11,50]. Oxygen flux in this study remained stable with microbial activity, suggesting that this form of management is a possibility, if the probability of metal dissolution is low, and will not contribute to AMD. Another possible issue with

AMD remediation sludge being used as an oxygen barrier is the potential for the sediment to dry and crack, which would cause preferential pathways for oxygen-rich waters to travel [10]. A solution to this, as noted by Zinck and Griffith (2005), is to apply either a vegetation cover or a water cap so that the sludge/sediment remains saturated.

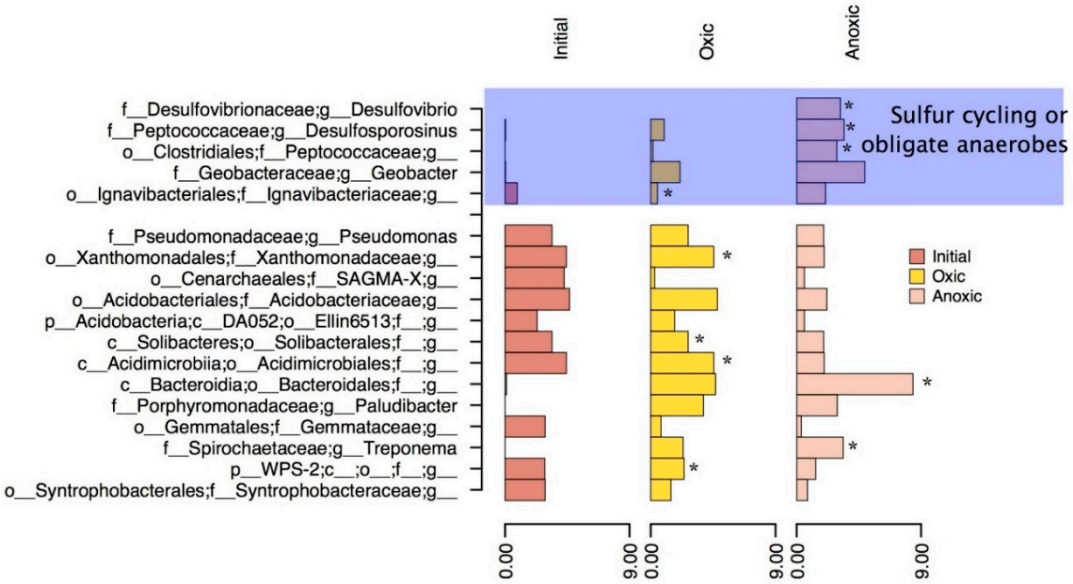

Figure 6. Most abundant Genera in the final oxic and anoxic timepoints, as well as the initial in situ bacteria. The asterisks represent genera that have significant differential abundant OTUs between the oxic and anoxic communities. The top blue section of the figure are Genera that have shown to be important for sulfur cycling or other obligate anaerobic pathways based on literature searches.

Differential abundant OTUs in the anoxic mesocosms were identified most commonly in the *Desulovibrio* and *Desulfosporosinus* genus (within *deltaproteobacteria* and *clostridia* classes respectively). The MSB sludge in this study showed a comparable increase in particles with high iron and sulfur concentrations after anoxic incubation which correlates to the abundant genera of SRB's observed. Genera such as *Desulovibrio* and *Desulfosprosinus* are abundant in this system (Figure 6) and can reduce sulfate using a dissimilatory reduction pathway to produce H_2S. These genera have been found in both AMD [51–55] and AMD remediation environments [56] in previous studies and are most likely responsible for the sulfide microcrystallites observed in the anoxic biotic incubations. For these reactions to occur there would have to be a source of low molecular weight organic carbon usually formed by the degradation of more complex molecules. The source of carbon in this system would most likely be from organic material and chitin left behind in shell fragments that would be inadvertently collected when removing the sediment/sludge layer. Bacteria such as *Pseudomonas* (5% of the sequences) could be responsible for the degradation of carbon, suggested by their high abundance in the current system and high metabolic diversity allowing them to survive in AMD environments [51,57–59]. *Pseudomonas* has been previously suggested to live in combination with SRB's within the deeper (and anoxic) sections of the MSB [31]. The anoxic incubation provided a way to test if the microbial community from the oxic portion of the bioreactor could thrive in an anoxic environment and if they increased the stability of the sediment/sludge in this environment. Since SRB's were present, and H_2S was produced and reacted to form a precursor to pyrite framboids, the microbes would cause an increased stability with regard to metal contamination if the sediment was placed in an anoxic environment, such as deep-pit burial. Anoxic zones are a more traditional method of storing mine wastes, either in the form of stockpiles or tailings ponds. Stockpiles can be effective if planned correctly, and currently are being used for waste rock storage on the mine site in this study.

4. Conclusions

Mussel shell bioreactors are an effective and inexpensive way to remediate AMD; however, depending on the area of their deployment, there is the potential for gradual accumulation of a sludge layer. The accumulation of sediment (e.g., alluvium and aeolian deposition) on the surface of the bioreactor is a limiting factor and requires management. AMD sludge management requires risk assessment of this secondary contamination for assessment of metal release and provides added information on whether the material can be actively repurposed. In this study, both anoxic and oxic storage mechanisms were investigated to evaluate the microbial impacts on the material. Storage of the sludge residue under oxic conditions increased soluble Mn, Al, and S phases. The presence of bacteria had a significant impact on the release of metals associated with oxyhydroxide mineral phases. These bacteria were an underlying factor in the low sediment oxygen demand (SOD) which resulted in steady state control of oxygen flux into the sediment. Although this material may be useful as an oxygen barrier over tailings or waste rock, there is still the possibility of metals being remobilized. Based on the results of this study, current repurposing of this AMD sludge should be applied to saturated circumneutral environments (e.g., wetlands, backfills, or under soil caps). These conclusions were further supported while investigating the stability of this material under anoxia. Storage of sludge material under anoxic conditions promotes the formation of iron sulfides, which immobilized the metals of concern at this location. Microbial community analyses indicated the presence of active SRB communities. This was further correlated with chemical measurements which showed measurable H_2S within the laboratory mesocosms associated with a shift in microbial community structure. Under conditions of anoxia, further evidence of increased metals associated with stable organic phases was also apparent. From a procedural perspective, burial mitigation may be the best solution to manage the AMD sludge.

Author Contributions: Conceptualization, C.G.W. and J.P.; formal analysis, S.C.B. and S.R.C.; investigation, S.C.B.; resources, C.G.W., J.P., D.D.H.; writing—original draft preparation, S.C.B.; writing—review and editing, C.G.W., J.P., D.D.H., S.C.B., S.R.C.; visualization, S.C.B.; supervision, C.H. and D.D.H.; project administration, C.G.W.; funding acquisition, C.G.W., J.P.

Funding: This research was funded in part by grants from the Natural Sciences and Engineering Council of Canada (NSERC) Discovery program 860006, ERASMUS CREATE grant 397997-2011, MITACS. IT08566 Global Partnership Award and funding provided by Bathurst Resources, O'Kane Consulting and New Zealand MBIE research contract 1403 held by CRL energy.

Acknowledgments: The authors would like to thank CRL energy for providing logistical support for this research, and Solid Energy for access to the mine site as well as Paul Weber for help in the field and project concept. Also, thanks for additional support from lab members including Daniel VanMensel and Thomas Reid for assistance in the field and sample preparation. Additional thanks to staff at GLIER including Sharon Mackie at the SEM facility, J.C. Barette for assistance with the ICPOES analyses, as well as Russel Hepburn in the genomics lab.

Conflicts of Interest: The authors declare no conflict of interest.

References

1. Bridge, G. CONTESTED TERRAIN: Mining and the Environment. *Annu. Rev. Environ. Resour.* **2004**, *29*, 205–259. [CrossRef]
2. Akcil, A.; Koldas, S. Acid Mine Drainage (AMD): Causes, treatment and case studies. *J. Clean. Prod.* **2006**, *14*, 1139–1145. [CrossRef]
3. Nordstrom, D.K. The rate of ferrous iron oxidation in a stream receiving acid mine effluent. *Sel. Pap. Hydrol. Sci.* **1985**, *1985*, 113–119.
4. Mayes, W.M.; Johnston, D.; Potter, H.A.B.; Jarvis, A.P. A national strategy for identification, prioritisation and management of pollution from abandoned non-coal mine sites in England and Wales. I.: Methodology development and initial results. *Sci. Total Environ.* **2009**, *407*, 5435–5447. [CrossRef] [PubMed]
5. Armitage, P.D.; Bowes, M.J.; Vincent, H.M. Long-term changes in macroinvertebrate communities of a heavy metal polluted stream: The river Nent (Cumbria, UK) after 28 years. *River Res. Appl.* **2007**, *23*, 997–1015. [CrossRef]

6. Han, Y.-S.; Youm, S.-J.; Oh, C.; Cho, Y.-C.; Ahn, J.S. Geochemical and eco-toxicological characteristics of stream water and its sediments affected by acid mine drainage. *Catena* **2017**, *148*, 52–59. [CrossRef]
7. Singer, P.C.; Stumm, W. Acidic Mine Drainage: The Rate-Determining Step. *Source Sci. New Ser.* **1970**, *167*, 1121–1123. [CrossRef]
8. Schippers, A.; Jozsa, P.-G.; Sand, W. Evaluation of the efficiency of measures for sulphidic mine waste mitigation. *Appl. Microbiol. Biotechnol.* **1998**, *49*, 698–701. [CrossRef]
9. DiLoreto, Z.A.; Weber, P.A.; Olds, W.; Pope, J.; Trumm, D.; Chaganti, S.R.; Heath, D.D.; Weisener, C.G. Novel cost effective full scale mussel shell bioreactors for metal removal and acid neutralization. *J. Environ. Manag.* **2016**. [CrossRef]
10. Zinck, J.; Griffith, W. CANMET Mining and Mineral Sciences Laboratories. *Mine Environ. Neutral Drain.* **2005**, *Report 3.43.1*, 1–60.
11. Demers, I.; Mbonimpa, M.; Benzaazoua, M.; Bouda, M.; Awoh, S.; Lortie, S.; Gagnon, M. Use of acid mine drainage treatment sludge by combination with a natural soil as an oxygen barrier cover for mine waste reclamation: Laboratory column tests and intermediate scale field tests. *Miner. Eng.* **2017**, *107*, 43–52. [CrossRef]
12. Macías, F.; Pérez-López, R.; Caraballo, M.A.; Cánovas, C.R.; Nieto, J.M. Management strategies and valorization for waste sludge from active treatment of extremely metal-polluted acid mine drainage: A contribution for sustainable mining. *J. Clean. Prod.* **2017**, *141*, 1057–1066. [CrossRef]
13. DiLoreto, Z.A.; Weber, P.A.; Weisener, C.G. Solid phase characterization and metal deportment in a mussel shell bioreactor for the treatment of AMD, Stockton Coal Mine, New Zealand. *Appl. Geochem.* **2016**, *67*, 133–143. [CrossRef]
14. Trumm, D.; Ball, J.; Pope, J.; Weisener, C. Passive Treatment of ARD Using Mussel Shells—Part III: Technology Improvement and Future Direction. In Proceedings of the 10th International Conference on Acid Rock Drain, IMWA Conference, Santiago, Chile, 21–24 April 2015; pp. 1–9.
15. McCauley, C.; O'Sullivan, A.; Weber, P.; Trumm, D. Variability of Stockton Coal Mine drainage chemistry and its treatment potential with biogeochemical reactors. *N. Z. J. Geol. Geophys.* **2010**, *53*, 211–226. [CrossRef]
16. Pope, J.; Weber, P.; Mackenzie, A.; Newman, N.; Rait, R. Correlation of acid base accounting characteristics with the Geology of commonly mined coal measures, West Coast and Southland, New Zealand. *N. Z. J. Geol. Geophys.* **2010**, *53*, 153–166. [CrossRef]
17. Weisener, C.; Weber, P. Preferential oxidation of pyrite as a function of morphology and relict texture. *N. Z. J. Geol. Geophys.* **2010**, *53*, 167–176. [CrossRef]
18. McCauley, C.A.; O'Sullivan, A.D.; Milke, M.W.; Weber, P.A.; Trumm, D.A. Sulfate and metal removal in bioreactors treating acid mine drainage dominated with iron and aluminum. *Water Res.* **2009**, *43*, 961–970. [CrossRef] [PubMed]
19. McCauley, C.; O'Sullivan, A.D.; Weber, P.; Trumm, D. Variability of Stockton Mine Acid Mine Drainage and Its Treatment Using Waste Substrates in Biogeochemical Reactors. Available online: https://ir.canterbury.ac.nz/handle/10092/4533 (accessed on 18 January 2019).
20. Chen, M.; Walshe, G.; Chi Fru, E.; Ciborowski, J.J.H.; Weisener, C.G. Microcosm assessment of the biogeochemical development of sulfur and oxygen in oil sands fluid fine tailings. *Appl. Geochem.* **2013**, *37*, 1–11. [CrossRef]
21. Reid, T.; Boudens, R.; Ciborowski, J.J.H.; Weisener, C.G. Physicochemical gradients, diffusive flux, and sediment oxygen demand within oil sands tailings materials from Alberta, Canada. *Appl. Geochem.* **2016**, *75*, 90–99. [CrossRef]
22. Boudens, R.; Reid, T.; VanMensel, D.; Prakasan, M.R.S.; Ciborowski, J.J.H.; Weisener, C.G. Bio-physicochemical effects of gamma irradiation treatment for naphthenic acids in oil sands fluid fine tailings. *Sci. Total Environ.* **2016**, *539*, 114–124. [CrossRef] [PubMed]
23. Revsbech, N.P. Diffusion characteristics of microbial communities determined by use of oxygen microsensors. *J. Microbiol. Methods* **1989**, *9*, 111–122. [CrossRef]
24. Unisense A/S. Website 2017. Available online: http://.unisense.com/ (accessed on 30 December 2018).
25. Revsbech, N.P.; Nielsen, L.P.; Ramsing, N.B. A novel microsensor for determination of apparent diffusivity in sediments. *Limnol. Oceanogr.* **1998**, *43*, 986–992. [CrossRef]

26. Diloreto, Z.A. Scholarship at UWindsor Biogeochemical Investigations of a Full Scale Mussel Shell Bioreactor for the Treatment of Acid Mine Drainage (AMD), the Stockton Mine, New Zealand. Master's Thesis, University of Windsor, Windsor, ON, Canada, 2016.
27. Ribeta, I.; Ptacek, C.J.; Blowes, D.W.; Jambor, J.L. The potential for metal release by reductive dissolution of weathered mine tailings. *J. Contam. Hydrol.* **1995**, *17*, 239–273. [CrossRef]
28. Fangueiro, D.; Bermond, A.; Santos, E.; Carapuça, H.; Duarte, A. Heavy metal mobility assessment in sediments based on a kinetic approach of the EDTA extraction: Search for optimal experimental conditions. *Anal. Chim. Acta* **2002**, *459*, 245–256. [CrossRef]
29. Heron, G.; Christensen, T.H.; Tjell, J.C. Oxidation Capacity of Aquifer Sediments. *Environ. Sci. Technol.* **1994**, *28*, 153–158. [CrossRef] [PubMed]
30. Amirbahman, A.; Schönenberger, R.; Johnson, C.A.; Sigg, L. Aqueous- and Solid-Phase Biogeochemistry of a Calcareous Aquifer System Downgradient from a Municipal Solid Waste Landfill (Winterthur, Switzerland). *Environ. Sci. Technol.* **1998**, *32*, 1933–1940. [CrossRef]
31. Falk, N.; Chaganti, S.R.; Weisener, C.G. Evaluating the microbial community and gene regulation involved in crystallization kinetics of ZnS formation in reduced environments. *Geochim. Cosmochim. Acta* **2018**, *220*, 201–216. [CrossRef]
32. Parada, A.E.; Needham, D.M.; Fuhrman, J.A. Every base matters: Assessing small subunit rRNA primers for marine microbiomes with mock communities, time series and global field samples. *Environ. Microbiol.* **2016**, *18*, 1403–1414. [CrossRef]
33. Edgar, R.C.; Haas, B.J.; Clemente, J.C.; Quince, C.; Knight, R. UCHIME improves sensitivity and speed of chimera detection. *Bioinformatics* **2011**, *27*, 2194–2200. [CrossRef]
34. Edgar, R.C. Search and clustering orders of magnitude faster than BLAST. *Bioinformatics* **2010**, *26*, 2460–2461. [CrossRef]
35. Love, M.I.; Huber, W.; Anders, S. Moderated estimation of fold change and dispersion for RNA-seq data with DESeq2. *Genome Biol.* **2014**, *15*, 550. [CrossRef] [PubMed]
36. Weiss, S.; Xu, Z.Z.; Peddada, S.; Amir, A.; Bittinger, K.; Gonzalez, A.; Lozupone, C.; Zaneveld, J.R.; Vázquez-Baeza, Y.; Birmingham, A.; et al. Normalization and microbial differential abundance strategies depend upon data characteristics. *Microbiome* **2017**, *5*, 27. [CrossRef] [PubMed]
37. Lloyd, M.; Ghelardi, R.J. A Table for Calculating the 'Equitability' Component of Species Diversity. *J. Anim. Ecol.* **1964**, *33*, 217. [CrossRef]
38. Chao, A. Nonparametric Estimation of the Number of Classes in a Population. *Scand. J. Stat.* **1984**, *11*, 265–270.
39. Thorbergsdóttir, I.M.; Reynir Gíslason, S.; Ingvason, H.R.; Einarsson, Á. Benthic oxygen flux in the highly productive subarctic Lake Myvatn, Iceland: In situ benthic flux chamber study. *Aquat. Ecol.* **2004**, *38*, 177–189. [CrossRef]
40. Wilkin, R.T.; Barnes, H.L. Formation processes of framboidal pyrite. *Geochim. Cosmochim. Acta* **1997**, *61*, 323–339. [CrossRef]
41. Frankel, R.B. Biologically Induced Mineralization by Bacteria. *Rev. Mineral. Geochem.* **2003**, *54*, 95–114. [CrossRef]
42. Gadd, G.M. Metals, minerals and microbes: Geomicrobiology and bioremediation. *Microbiology* **2010**, *156*, 609–643. [CrossRef] [PubMed]
43. Ferris, F.G.; Tazaki, K.; Fyfe, W.S. Iron oxides in acid mine drainage environments and their association with bacteria. *Chem. Geol.* **1989**, *74*, 321–330. [CrossRef]
44. Gadde, R.R.; Laitinen, H.A. Studies of Heavy Metal Adsorption by Hydrous Iron and Manganese Oxides. *Anal. Chem.* **1974**, *46*, 2022–2026. [CrossRef]
45. Lee, G.; Bigham, J.M.; Faure, G. Removal of trace metals by coprecipitation with Fe, Al and Mn from natural waters contaminated with acid mine drainage in the Ducktown Mining District, Tennessee. *Appl. Geochem.* **2002**, *17*, 569–581. [CrossRef]
46. Tessier, A.; Rapin, F.; Carignan, R. Trace metals in oxic lake sediments: Possible adsorption onto iron oxyhydroxides. *Geochim. Cosmochim. Acta* **1985**, *49*, 183–194. [CrossRef]
47. Liao, P.; Li, W.; Jiang, Y.; Wu, J.; Yuan, S.; Fortner, J.D. Formation, Aggregation, and Deposition Dynamics of NOM-Iron Colloids at Anoxic–Oxic Interfaces. *Environ. Sci. Technol.* **2017**, *51*, 12235–12245. [CrossRef] [PubMed]

48. Clark, D.A.; Norris, P.R. *Acidimicrobium ferrooxidans* gen. nov., sp. nov.: Mixed-culture ferrous iron oxidation with Sulfobacillus species. *Microbiology* **1996**, *142*, 785–790. [CrossRef]
49. Schwertmann, U. Solubility and dissolution of iron oxides. *Plant Soil* **1991**, *130*, 1–25. [CrossRef]
50. Demers, I.; Benzaazoua, M.; Mbonimpa, M.; Bouda, M.; Bois, D.; Gagnon, M. Valorisation of acid mine drainage treatment sludge as remediation component to control acid generation from mine wastes, part 1: Material characterization and laboratory kinetic testing. *Miner. Eng.* **2015**, *76*, 109–116. [CrossRef]
51. Sánchez-Andrea, I.; Sanz, J.L.; Bijmans, M.F.M.; Stams, A.J.M. Sulfate reduction at low pH to remediate acid mine drainage. *J. Hazard. Mater.* **2014**, *269*, 98–109. [CrossRef]
52. Méndez-García, C.; Peláez, A.I.; Mesa, V.; Sánchez, J.; Golyshina, O.V.; Ferrer, M. Microbial diversity and metabolic networks in acid mine drainage habitats. *Front. Microbiol.* **2015**, *6*, 475.
53. Schippers, A.; Breuker, A.; Blazejak, A.; Bosecker, K.; Kock, D.; Wright, T.L. The biogeochemistry and microbiology of sulfidic mine waste and bioleaching dumps and heaps, and novel Fe(II)-oxidizing bacteria. *Hydrometallurgy* **2010**, *104*, 342–350. [CrossRef]
54. Florentino, A.P.; Weijma, J.; Stams, A.J.M.; Sánchez-Andrea, I. Sulfur Reduction in Acid Rock Drainage Environments. *Environ. Sci. Technol.* **2015**, *49*, 11746–11755. [CrossRef]
55. Barton, L.L.; Hamilton, A. *The Sulphate-Reducing Bacteria*; Cambridge University Press: New York, NY, USA, 2007; Volume 1542, ISBN 9780511541490.
56. Lee, Y.-J.; Romanek, C.S.; Wiegel, J. *Desulfosporosinus youngiae* sp. nov., a spore-forming, sulfate-reducing bacterium isolated from a constructed wetland treating acid mine drainage. *Int. J. Syst. Evol. Microbiol.* **2009**, *59*, 2743–2746. [CrossRef]
57. Bruneel, O.; Mghazli, N.; Hakkou, R.; Dahmani, I.; Filali Maltouf, A.; Sbabou, L. In-depth characterization of bacterial and archaeal communities present in the abandoned Kettara pyrrhotite mine tailings (Morocco). *Extremophiles* **2017**, *21*, 671–685. [CrossRef] [PubMed]
58. Wakeman, K.D.; Erving, L.; Riekkola-Vanhanen, M.L.; Puhakka, J.A. Silage supports sulfate reduction in the treatment of metals- and sulfate-containing waste waters. *Water Res.* **2010**, *44*, 4932–4939. [CrossRef] [PubMed]
59. Martins, M.; Faleiro, M.L.; Silva, G.; Chaves, S.; Tenreiro, R.; Costa, M.C. Dynamics of bacterial community in up-flow anaerobic packed bed system for acid mine drainage treatment using wine wastes as carbon source. *Int. Biodeterior. Biodegrad.* **2011**, *65*, 78–84. [CrossRef]